Bulletin of Mathematical Biology (1998) **60**, 477–503

Models for the Length Distributions of Actin Filaments: II. Polymerization and Fragmentation by Gelsolin Acting Together

G. BARD ERMENTROUT
Department of Mathematics,
University of Pittsburgh
Pittsburgh, PA 15260, U.S.A.

LEAH EDELSTEIN-KESHET*
Department of Mathematics,
University of British Columbia,
Vancouver, BC,
Canada, V6T 1Z2

In a previous paper, we studied elementary models for polymerization, depolymerization, and fragmentation of actin filaments (Edelstein-Keshet and Ermentrout, 1998, *Bull. Math. Biol.* **60**, 449–475). When these processes act together, more complicated dynamics occur. We concentrate on a particular case study, using the actin-fragmenting protein gelsolin. A set of biological parameter values (drawn from the experimental literature) is used in computer simulations of the kinetics of gelsolin-mediated actin filament fragmentation.

© *1998 Society for Mathematical Biology*

1. Glossary of Parameters

Many of the parameters associated with polymerization and fragmentation have been defined in our previous paper (Edelstein-Keshet and Ermentrout, 1998). We include them below.

G_j	An actin filament with j monomers and a gelsolin cap at its barbed end.
$x_j = [G_j], a$	Concentration of gelsolin-capped actin j-mers, of actin monomers.
k_+, k_-	Polymerization, depolymerization rate constants for actin.
k_g	Rate of binding to and severing of an actin filament by gelsolin.
g	Concentration of free gelsolin.

*Author to whom correspondence should be addressed.

0092-8240/98/030477 + 27 $25.00/0 bu970012 © 1998 Society for Mathematical Biology

a	Concentration of free actin.
k_{init}	Gelsolin-induced rate of nucleation of actin filament from monomers.
k_{g2}	Rate of breakdown of the gelsolin–(actin)$_2$ complex to two gelsolin-actin complexes.
k_2^-	Rate of breakdown of the gelsolin–(actin)$_2$ to monomeric actin plus gelsolin-actin.
k_{fast}	Rate of formation of gelsolin–(actin)$_2$ from gelsolin–actin.
κ	$=gk_g/k_-$ (dimensionless parameter when g is held fixed).
r	$=k_+a/k_-$ (dimensionless parameter when a is held fixed).
ρ	$= k_2^-/k_-$ (dimensionless parameter).
ι	$= gk_{init}/k_-$ (dimensionless parameter when g is held fixed).
a_∞	steady state concentration of free actin.
a_{crit}	k_-/k_+.
$\bar{\ell}$	mean length of filaments

2. Introduction

In this paper we explore the effect of competing processes, polymerization and fragmentation, when they act together on the length distribution of actin filaments. Although filament annealing (joining together of two pieces) may also be an important process, we will not include it explicitly in this paper. Our previous paper developed a formalism and some analytic results for simpler models in which only one of the two processes was operating. We now consider *gelsolin*, which causes fragmentation of filaments, and other effects that both promote and inhibit polymerization. Even though it is not possible to include all the biological detail in a first modeling treatment such as this one, we have made an effort, in this paper, to document current biological knowledge regarding the effects of gelsolin-like proteins on actin, and to point the interested reader to the relevant literature. We focus on the specific case of gelsolin for the following reasons.

1. Gelsolin is prominent among the actin-binding proteins and occurs in a wide variety of cells (Kwiatkowski, 1988; Howard *et al.*, 1990; Hartwig and Kwiatkowski, 1991). Its kinetics and effects on the actin molecule have been studied and detailed information is available (Schoepper and Wegner, 1992; Ditsch and Wegner, 1994, 1995).
2. Gelsolin has a variety of effects including nucleation, filament capping, and filament fragmentation. A quantitative model is desirable to understand these competing and synergetic effects.
3. The relative importance of actin filament elongation, nucleation, and fragmentation in the regulation of cell motility is still unclear (Redmond and Zigmond, 1993; Zigmond, 1993; Theriot, 1994; Lauffenburger and Horowitz, 1996; Mitchison and Cramer, 1996). Theoretical analysis may help to tease

apart competing hypotheses. For example, the role of gelsolin and similar proteins that fragment actin filaments is still under investigation (Redmond and Zigmond, 1993; Lauffenburger and Horowitz, 1996).

4. In the respiratory disease cystic fibrosis (CF), cells in the lungs die, spilling a highly viscous solution containing long actin filaments into a patient's lungs. Actin-fragmenting proteins such as gelsolin are currently being investigated as a potential treatment to help reduce airway mucus viscosity and alleviate symptoms. Thus, the effect of gelsolin on actin filament length distribution is of interest from both a basic and an applied science perspective (Vasconcellos *et al.*, 1994; Biogen, 1996; McGough, 1997).

In this paper we first comment on how a small amount of breakage or fragmentation influences the size distribution formed by polymerization and depolymerization kinetics. Some approximation techniques (asymptotic methods) then give an indication of the expected behavior.

The case of gelsolin is described in a full model consisting of differential equations for the filament size classes. In many cases, we can determine the exact steady-state behavior of the models. However, we do not have a closed-form solution for the transient behavior, which can be quite interesting, and so we concentrate on numerical solutions of the evolution problem.

3. Proteins that Fragment Actin Filaments

A number of proteins have been identified as actin-filament-severing agents. One family of actin-cutting proteins is the calcium-sensitive *gelsolin* family, which includes *gelsolin*, *villin* (80 kDa), *severin*, *fragmin* (40 kDa), *brevin* (which does not actually sever actin) and *β-actinin*. Of particular relevance to this paper is the role of gelsolin, but some detailed references for gelsolin and for other fragmenting proteins are organized by subject in Appendix 1 for the convenience of the reader.

Gelsolin is found in cells of mammals, birds, and amphibians. Its ubiquitous distribution means that it is among the more well-studied and characterized of the fragmenting proteins. Gelsolin has a variety of important actions on actin monomers and filaments (Howard *et al.*, 1990; Schoepper and Wegner, 1991, 1992; Laham *et al*., 1993; Ditsch and Wegner, 1994, 1995). Gelsolin is known to cut actin filaments, cap the barbed end of an actin filament, bind free actin monomers, and nucleate actin polymerization. Gelsolin generally stays attached to the new barbed end that is formed when it cuts a preexisting actin filament. This means that under many circumstances gelsolin is not a 'recycled' fragmenter, as it has a rather slow rate of dissociation from the cut filament.

Another fragmenting protein that is also distributed widely among eucaryotes is *cofilin*. Like gelsolin, it exhibits the ability to bind monomers and filaments, and to cut filaments. Unlike gelsolin, it does not stay attached to a filament that

it severs, and is a prototype of a 'recyclable' fragmenter (Maciver *et al.*, 1991; Hawkins *et al.*, 1993; Hayden *et al.*, 1993; Moon and Drubin, 1995; Aizawa *et al.*, 1996). The effect of this type of recycled fragmenter was modeled and described in Edelstein-Keshet and Ermentrout (1998).

The functions of gelsolin are regulated by calcium, which must be present in micromole concentrations to allow filament nucleation, and in larger quantities to cause filament severing (Howard *et al.*, 1990; Yin *et al.*, 1990; Hartwig and Kwiatkowski, 1991). The membrane polyphosphoinositides (*PIPs*) such as phosphatidylinositol 4,5-biphosphate, (PIP_2) are important players in signal transduction pathways and affect the ability of gelsolin to cap and cut actin filaments. Although we shall not be concerned here with the higher levels of organization in the cell, this suggests a variety of fine-tuned controls on the processes that lead to changes in polymerization, filament lengths, and gellation in the cytoskeleton. Details of the processes actually occurring *in vivo* are still shrouded in mystery.

As indicated in the Introduction, gelsolin is now being used as a promising direct treatment for the symptoms of CF. Its important effect there is on the long actin filaments deposited on the lung surface when cells of the immune system die. Biogen has recently announced phase I clinical trials of gelsolin as an agent that severs these actin filaments, thereby reducing mucus viscosity, allowing it to be more easily expelled by the patient (Biogen, 1996). This attests to the importance of understanding gelsolin (Stossel, 1994), its structure and actions (McGough, 1997), and its effect on actin filament length distribution.

4. How Gelsolin Affects Polymerization and Fragmentation

The functions of gelsolin that we incorporate into the model are summarized below.

1. Gelsolin can nucleate actin filaments from two monomers (Ditsch and Wegner, 1994). However, the rate-limiting step is the formation of the gelsolin:actin 1:1 complex, with a very rapid binding of the second monomer (Selve and Wegner, 1987). In this respect, in the presence of gelsolin, filament initiation differs from its nucleation when only actin monomers are present. Nucleation is experimentally found to occur at a rate that is roughly linear in actin monomer concentration.
2. Gelsolin binds to and fragments an actin filament.
3. Gelsolin stays attached, i.e., caps the barbed end of an actin filament. The filament can still polymerize or lose monomers from its slower-growing pointed end.

The rates of the reactions, and their sensitivity to calcium and other conditions were studied *in vitro* by Selve and Wegner (1987), Ditsch and Wegner (1994, 1995), Schoepper and Wegner (1991, 1992) (Table 1). In these experiments, actin was initiated predominately by gelsolin, so that all growing filaments were

capped at their barbed ends. As Ditsch and Wegner (1994) were interested in characterizing kinetic rates and sigmoidal reaction kinetics rather than length distributions, the total amount of gelsolin in their experiments was kept rather low, at 10 nM = 0.01 μM.

Table 1. Rate constants for actin–gelsolin interactions. The polymerization rates reflect growth at the pointed end of the actin filament since the barbed end is capped.

Parameter	Value	Units	Meaning	Source
k_g	3.0	$\mu M^{-1}\ s^{-1}$	Fragmentation rate, gelsolin	Ditsch and Wegner (1994)
k_+	0.5	$\mu M^{-1}\ s^{-1}$	Polymerization rate (p end)	Ditsch and Wegner (1994)
	0.28			Selve and Wegner (1986)
k_-	0.32	s^{-1}	Depolymerization rate (p end)	Ditsch and Wegner (1994)
	0.2			Selve and Wegner (1986)
k_{init}	2.5×10^{-2}	$\mu M^{-1}\ s^{-1}$	Filament initiation rate, gelsolin	Selve and Wegner (1987)
k_{init}	1.5×10^{-2}	$\mu M^{-1}\ s^{-1}$		Ditsch and Wegner (1994)
k_{init}	2.1×10^{-2}	$\mu M^{-1}\ s^{-1}$		Laham *et al.* (1993)
k_{fast}	20	$\mu M^{-1}\ s^{-1}$	Formation of G_2 from G_1	Schoepper and Wegner (1991)
k_{g2}	—	$\mu M^{-1}\ s^{-1}$	Fragmentation of G_2	
k_2^-	0.02	s^{-1}	Depolymerization of G_2	Schoepper and Wegner (1991)
g	0.01	μM	Gelsolin concentration	Ditsch and Wegner (1994)
a	0.1–2.0	μM	Actin concentration	
r	0.16–3.2	Dimensionless	k_+a/k_-	calculated for gelsolin
κ	0.1		gk_g/k_-	using values from
ι	5×10^{-4}		gk_{init}/k_-	Ditsch and Wegner (1994)
ρ	0.0–0.1		k_2^-/k_-	

We use the notation G_j to denote an actin filament with j monomers and a gelsolin cap at its barbed end. The symbols a and g denote both the free actin and gelsolin, respectively, and their concentrations. The appropriate set of chemical reactions is as follows.

Gelsolin-mediated nucleation

$$G + a \overset{k_{init}}{\rightarrow} G_1. \tag{1}$$

$$G_1 + a \overset{k_{fast}}{\rightarrow} G_2. \tag{2}$$

Polymerization and depolymerization at the pointed end

$$G_j + a \underset{k_-}{\overset{k_+}{\rightleftharpoons}} G_{j+1}. \tag{3}$$

Gelsolin-caused fragmentation

$$G_{j+k} + g \overset{k_g}{\rightarrow} G_j + G_k. \tag{4}$$

In the first two reactions, gelsolin forms a complex with an actin monomer (rate k_{init}). This complex then reacts quickly with a second actin monomer to form a gelsolin:actin 1:2 complex (rate k_{fast}) (Schoepper and Wegner, 1991).

Many of the parameter values associated with these reaction kinetics are known. These have been collected in Table 1, together with some of the dimensionless parameter groupings that will appear in the model.

In deriving the equations of the model, we let x_j represent the concentration of G_j, i.e., of filaments with one gelsolin cap and j actin monomers. We note that, as in our previous paper, if a filament has j actin monomers, there are $j-1$ bonds at which it can be broken. For example consider $G_5 = Gaaaaa$, which can become $Gaaaa + Ga$, $Gaaa + Gaa$, $Gaa + Gaaa$, and $Ga + Gaaaa$. Observe that two copies of each type of product can be formed. Thus, as a result of chopping, the rate of change of x_k will have terms of the form:

$$k_g g\left(2\sum_{k=j+1}^{N} x_k - (j-1)x_j\right).$$

We first develop the equations that describe the initiation process, since this involves special consideration of different time scales of formation of the 1:1 and 1:2 complexes. If gelsolin:actin 1:2 intermediate ('dimer' gaa) is fragmented, it would only break into a pair of ga intermediates which have a very short lifetime. (One can eliminate this reaction entirely if desired; the rate k_{g2} is used to distinguish it from the other fragmentation reactions.) We further denote the depolymerization of dimers with the rate constant k_2^- (which can also be set to zero). Consider the intermediates G_1, G_2 and the free actin whose respective concentrations are x_1, x_2 and a. The equations that describe these would have the general forms:

$$\frac{da}{dt} = -k_{fast}ax_1 + \text{other terms} \tag{5}$$

$$\frac{dx_1}{dt} = -k_{fast}ax_1 + k_{init}ag + k_2^- x_2 + 2gk_{g2}x_2 + 2k_g g\sum_{j=3}^{N} x_j \tag{6}$$

$$\frac{dx_2}{dt} = k_{fast}ax_1 - k_2^- x_2 - 2gk_{g2}x_2 + \text{other terms} \tag{7}$$

where the 'other terms' are independent of x_1. The term $k_2^- x_2$ represents any spontaneous decay of the complex G_2 into G_1 and a, while the term $2gk_{g2}x_2$ represents any active cutting of such a complex by gelsolin. If this were to occur, it would create two equal pieces, both of the type G_1. These terms are included for generality, but their rate constants can be set to zero or to very low values where such reactions are rare or nonexistent. The summation term describes small G_1-sized pieces that are chopped off larger filaments.

Since k_{fast} is very large, the concentration of x_1 will be small ($O(1/k_{fast})$) so we will replace the term $k_{fast}ax_1$ by its steady-state value:

$$k_{fast}ax_1 = k_{init}ag + k_2^- x_2 + 2gk_{g2}x_2 + 2k_g g \sum_{j=3}^{N} x_j \equiv R_1.$$

By this procedure, we eliminate x_1 from the equations. We now collect all reaction terms in the set of equations that describe the above system:

$$\frac{dg}{dt} = -k_{init}ga - gk_{g2}x_2 - gk_g \sum_{j=3}^{N}(j-1)x_j \tag{8}$$

$$\frac{da}{dt} = -R_1 + k_2^- x_2 - k_{init}ga - k_+ a \sum_{j=2}^{N-1} x_j + k_- \sum_{j=3}^{N} x_j \tag{9}$$

$$\frac{dx_2}{dt} = R_1 - k_2^- x_2 - gk_{g2}x_2 - k_+ ax_2 + k_- x_3 + 2k_g g \sum_{j=3}^{N} x_j \tag{10}$$

$$\vdots = \vdots \tag{11}$$

$$\frac{dx_j}{dt} = k_+ a(x_{j-1} - x_j) + k_-(x_{j+1} - x_j) + k_g g\left(2\sum_{k=j+1}^{N} x_k - (j-1)x_j\right) \tag{12}$$

$$\vdots = \vdots \tag{13}$$

$$\frac{dx_N}{dt} = k_+ ax_{N-1} - k_- x_N - k_g g(N-1)x_N. \tag{14}$$

The equation for gelsolin includes depletion in all the above chemical processes, including formation of the 1:1 gelsolin:actin complex, and fragmentation and binding to all filaments. The actin monomer equation includes terms for reaction with the 1:1 complex, depolymerization and breakage of the 1:2 complex (which we may set to zero), depletion through polymerization and recovery by depolymerization from all bigger filaments. A similar balance appears in the equation for x_2. These three equations are specific to the gelsolin–actin system, although we have allowed some room for generality. The equation for x_j contains terms for breakage and for polymerization, and combines features of the models for these individual processes discussed separately in our previous paper (Edelstein-Keshet and Ermentrout, 1998). The equation for x_N, a 'largest-size filament,' is included here for the purpose of numerical simulation.

Remarks. 1. The elimination of x_1 is valid because k_{fast} is large. However, if the actin concentration is small, then the term $k_{fast}a$ multiplying x_1 may

not be large; in this case we must include the full dynamics for the x_1 intermediate.

2. We can eliminate the last equation if we want to consider arbitrarily large polymers.
3. It is a simple matter to verify that the equations above conserve total actin, A_{total}, and total gelsolin G_{total}:

$$\frac{d}{dt}(g(t) + \sum_{j=2}^{N} x_j) \equiv \frac{dG_{total}}{dt} = 0, \tag{15}$$

Thus, $G_{total} = g(0)$, since we assume that at the beginning of the reaction the only form of actin is free monomers. Similarly,

$$A_{total} = a(t) + \sum_{j=2}^{N} j x_j \tag{16}$$

is constant and equal to $a(0)$ the total initial actin concentration.

5. Submodels and Simpler Variants

The equations given above include many effects and are difficult to study directly. We consider several simpler variants that describe special cases.

5.1. ***Steady state of full model when actin and gelsolin are conserved.*** In general, the initial molar ratio of free actin and gelsolin is much greater than 1. In this case, we can show that the gelsolin will be completely depleted, i.e., $g(t) \to 0$ as $t \to \infty$. Suppose that $k_{g2} = k_g$. Recall from equation (8),

$$\frac{dg}{dt} = -gk_g \left(\frac{k_{init}}{k_g} a + x_2 + \sum_{j=3}^{N} (j-1) x_j \right).$$

The terms inside the parentheses are clearly greater than $\sum_{j=2}^{N} x_j$ which is just $g(0) - g$ by conservation. Thus

$$\frac{dg}{dt} < -k_g g(g(0) - g)$$

and since $g(0) > 0$ this implies $g(t) \to 0$ as $t \to \infty$. (We assumed that $k_{g2} = k_g$ for this calculation. If that is not the case, the analysis is a little more complicated, but the result is the same.) Note that if $a(0)$ is small compared to $g(0)$ then this calculation is no longer valid since monomeric actin will be depleted before free gelsolin is depleted and all the x_j will tend to 0 (for $j \geq 2$).

Since the gelsolin is depleted, in the steady state, all terms in the equation which involve gelsolin will disappear. The steady-state equations are then:

$$
\begin{aligned}
0 &= -k_+ a x_2 + k_- x_3 \\
\vdots &= \vdots \\
0 &= k_+ a (x_{j-1} - x_j) + k_- (x_{j+1} - x_j) \\
\vdots &= \vdots \\
0 &= k_+ a x_{N-1} - k_- x_N .
\end{aligned}
$$

Note that the k_2^- term cancels owing to the fast polymerization of the G_1 complex. Thus, we are back to the case of polymerization acting alone (Edelstein-Keshet and Ermentrout, 1998). The solution to this difference equation is:

$$x_j = B(k_+ a / k_-)^j .$$

The constants in this expression, B and a, the steady-state free-actin concentration, are to be determined from the constraints on the total gelsolin and the total actin. We show the detailed procedure in Appendix 2, and conclude that if $r(0) = (k_+ a(0)/k_-) > 1$ which is the criterion for growth of the filaments, the mean length of filaments will be:

$$\bar{\ell} = \frac{\sum_{j=2}^{\infty} j x_j}{\sum_{j=2}^{\infty} x_j} = \frac{a(0) - a_\infty}{g(0)} .$$

Here, a_∞ is the steady-state actin concentration. By definition of r, we see that $a_\infty = k_-/k_+ r$. For small gelsolin concentrations, $r \approx 1$ (see Appendix 2) so that $a_\infty \approx k_-/k_+ = a_{crit}$ which gives a simple intuitively appealing expression for the mean length:

$$\bar{\ell} \approx \frac{a(0) - a_{crit}}{g(0)} . \tag{17}$$

As one would expect, the larger the initial concentration of gelsolin, the smaller the mean length of the filaments.

These calculations have all been for the case $N \to \infty$. For a finite cut-off in polymer size, the qualitative results are the same as long as N is big compared to the mean length expression above. If the cut-off in total length is too small, then it is possible for the distribution to be monotone increasing.

5.2. ***Low actin or high gelsolin.*** When the initial actin concentration is low, then the pseudosteady-state hypothesis we discussed above is no longer valid (see the remarks). What happens then is that *even if* k_{fast} *is very big* all the polymers

tend to 0 and only the ga complexes remain. (If k_2^- and k_{g2} are both zero then only the dimers remain, however, if either is nonzero then only the ga complex remains.)

It is easy to see that $g_\infty = g(0) - a(0)$ and $x_1 = a(0)$, where x_1 is the concentration of the ga complex. If both the dimer breakdown rates are 0 then $x_2 = a(0)/2$. All actin is either incorporated into the ga complex or the gaa complex if the latter does not break down.

5.3. ***Free actin monomer and gelsolin artificially held constant.*** This corresponds to what we called the *in vivo* case (Edelstein-Keshet and Ermentrout, 1998). In this case the total actin and the total gelsolin are not conserved but are buffered so, to be held constant. The system of equations is simply

$$\begin{aligned}
\frac{dx_1}{dt} &= k_{init}ag - k_{fast}ax_1 + k_2^- x_2 + 2k_g g \sum_{k>2} x_k \\
\frac{dx_2}{dt} &= k_{fast}ax_1 - k_2^- x_2 - k_+ ax_2 + k_- x_3 + 2k_g g \sum_{k>2} x_k \\
\vdots &= \vdots \\
\frac{dx_j}{dt} &= k_+ a(x_{j-1} - x_j) + k_-(x_{j+1} - x_j) + k_g g\left(2\sum_{k>j} x_k - (j-1)x_j\right) \\
\vdots &= \vdots \\
\frac{dx_N}{dt} &= k_+ ax_{N-1} - k_- x_N - k_g g(N-1)x_N.
\end{aligned}$$

Since a, g are just parameters in these equations, this is now a linear system. We can divide by k_- and rescale time. Define $\kappa = k_g g/k_-$, $r = k_+ a/k_-$, $\rho = k_2^-/k_-$, $\iota = k_{init}ag/k_-$, and $K = k_{fast}a/k_-$. For constant a, g, these are constant parameters. κ represents the rate of fragmentation by gelsolin relative to the rate of actin depolymerization. In the following sections we will use this dimensionless quantity to study the effect of a small amount of fragmentation. We get the following:

$$x_1' = \iota - Kx_1 + \rho x_2 + 2\kappa \sum_{l>2} x_l \tag{18}$$

$$x_2' = Kx_1 - \rho x_2 - rx_2 + x_3 + 2\kappa \sum_{l>2} x_l \tag{19}$$

$$\vdots = \vdots \tag{20}$$

$$x_j' = r(x_{j-1} - x_j) + x_{j+1} - x_j + \kappa\left(\sum_{l>j} x_l - (j-1)x_j\right) \tag{21}$$

$$\vdots = \vdots \tag{22}$$

$$x_N' = r x_{N-1} - x_N - \kappa(N-1)x_N \tag{23}$$

where x' means the derivative of x with respect to the dimensionless time, $k_{-}t$. Since this system does not go to steady state, it makes no sense to eliminate the x_1 equation and thus we retain it here. Though the system is linear, the summation terms and the size-dependent coefficients make it difficult to solve in closed form. In the next section, we show that all concentrations grow exponentially in time. We then use numerical solutions of this to look at relative distributions of the lengths of the filaments.

5.4. ***No free gelsolin.*** In this case there is no fragmentation taking place and no further initiation of new filaments. This is equivalent to setting $\kappa = 0$ so that the dimensionless equations have the form:

$$x_1' = -K x_1 + \rho x_2 \tag{24}$$

$$x_2' = K x_1 - \rho x_2 - r x_2 + x_3 \tag{25}$$

$$\vdots = \vdots \tag{26}$$

$$x_j' = r(x_{j-1} - x_j) + x_{j+1} - x_j \tag{27}$$

$$\vdots = \vdots \tag{28}$$

$$x_N' = r x_{N-1} - x_N \tag{29}$$

In absence of initiation, $K = 0, \rho = 0$, this system closely resembles a simple-polymerization system (Edelstein-Keshet and Ermentrout, 1998) and $x_j = 0$ is a rest state. The entries in the columns of the linearized matrix (just the coefficients of the x_j, since this is a linear system) all sum to 0 so that 0 is an eigenvalue. Furthermore, due to the tridiagonal nature of the model, if $r \neq 1$ then 0 is a simple eigenvalue, and from the Gerschgorin theorem (Horn and Johnson, 1985) all other eigenvalues have negative real parts. We can compute the eigenvector for the zero eigenvalue. By direct substitution it is easy to show that this eigenvector is

$$\Phi \equiv (1/K, 1, r, r^2, \ldots, r^{N-2})^T. \tag{30}$$

We will use this result in the perturbation calculation in the next section. We show that, even in absence of a source term, there will be exponential growth of all polymers as soon as $\kappa > 0$.

6. The Effect of a Low Level of Fragmentation

We now use a perturbation argument to show that exponential growth of polymers takes place as soon as fragmentation occurs, i.e., when $\kappa > 0$. The end result of the calculation (which may be skipped) is that there is exponential growth of all the filaments given approximately by

$$x_j(t) \approx r^{j-1} e^{k_g g \lambda_1 t}$$

where λ_1 is a positive expression given below [equation (31)].

To see this, we look at the perturbation of the 0 eigenvalue for small κ. The other negative eigenvalues will remain negative for small κ. Let A be the matrix for the $N \times N$ system when $\kappa = 0$. Then we know that $A\Phi = 0$ since Φ is the eigenvector with zero eigenvalue for A. Since the columns of A sum to zero, the eigenvector for A^T is

$$\Phi^* = (1, \ldots 1)^T.$$

Let B be the matrix associated with the fragmentation terms. Thus, the matrix for the full system is

$$M = A + \kappa B.$$

We will show that for small κ the zero eigenvalue is perturbed to a positive eigenvalue. Let $\phi(\kappa)$ be the κ-dependent eigenvector of M corresponding to eigenvalue $\lambda(\kappa)$, where $\lambda(0) = 0$ and $\phi(0) = \Phi$. Consider:

$$M(\kappa)\phi(\kappa) = \lambda(\kappa)\phi(\kappa)$$

Differentiate this with respect to κ, set $\kappa = 0$ and let $\Phi_1 = d/d\kappa\phi(\kappa)|_{\kappa=0}$;similarly define λ_1 as the derivative of λ at $\kappa = 0$. Then we get:

$$A\Phi_1 + B\Phi = \lambda_1\Phi.$$

Since A has a one-dimensional nullspace, we can find Φ_1 if and only if $Z \equiv -B\Phi + \lambda_1\Phi$ is in the range of A. The Fredholm alternative implies that for Z to be in the range, $\Phi^* \cdot Z = 0$. This uniquely determines λ_1, the lowest order perturbation of the zero eigenvalue:

$$\lambda_1 = \frac{\sum_{j=3}^{N} j r^{j-2}}{1/K + \sum_{j=0}^{N-2} r^j}. \tag{31}$$

This is clearly positive and thus we see that as soon as choppers are added, if the total actin and gelsolin are buffered to remain at a constant level, then a small initial dimer concentration will grow due to polymerization; chopping will then add more, etc. Clearly this positive feedback system grows. The mean length

and mass will remain bounded since they depend on ratios, and the exponential growth will cancel out.

In the absence of choppers ($\kappa = 0$), but with a source term, we can expect growth of the total population in time. Furthermore, the growth will be linear in time. The end result of such a calculation is that

$$x_j(t) \approx x_j^0 + ct$$

where x_j^0 is constant and c is proportional to ι.

We can show this by solving the differential equation:

$$\frac{dX}{dt} = AX + (\iota, 0, \ldots, 0)^T.$$

By the method of undetermined coefficients, we expect a solution of the form:

$$X(t) = X_0 + ct\Phi$$

where X_0 is a constant and c is unknown. Plugging this into the differential equations, we see:

$$c\Phi = AX_0 + (\iota, 0, \ldots, 0)^T.$$

Once again, appealing to the Fredholm alternative, we obtain:

$$c = \frac{\iota}{1/K + \sum_{j=0}^{N-2} r^j}.$$

Thus, a source term leads to linear growth in time. In the next section, we do some numerical simulations that confirm this analysis and also yield steady-state distributions.

7. Numerical Investigation of the Gelsolin Problem

We numerically investigate the system of equations of the full model. If we are interested in filament lengths up to several tens of monomers long, we can directly simulate the system of differential equations (6), and (8)–(14) with parameter values given in Table 1. If, however, we want to describe how filaments with hundreds of monomer units grow, the problem as formulated above becomes too cumbersome to treat numerically in an efficient manner.

In the biologically interesting situations, actin filaments can develop lengths of up to several microns. Since each 1 μ filament is composed of about 370 actin monomers, this means that we must find ways of describing a distribution of filaments when the maximal size class is in the order of 1000 monomers long. In this case, it is clearly unrealistic to keep track of individual j-mers for

$j = 1 \ldots 1000$, which would lead to a system of 1000 differential equations. For this reason, we replace the discrete model by a continuum equation (Edelstein-Keshet and Ermentrout, 1998) and then choose a new discretization which lumps together certain size classes. This yields a system which is amenable to numerical simulation. (We need to do this only in cases where there is expected to be growth of the larger filaments. When the larger filaments do not grow, they have a negligible effect on the solutions to the equations.)

Suppose that, in the continuum model, we have chosen δ to represent the 'mass' of a monomer. Let us now look at 'chunks' that consist of pieces that are larger than a single monomer, say of mass Δ. Then, by looking at the continuum model, we see that the rate constants for polymerization will be scaled by δ/Δ and those for the chopping will be scaled by Δ/δ. (This follows by 'rediscretizing' the continuum model using Δ instead of δ as the 'ds'.) That is, k_+, k_- are divided by the ratio of $M \equiv \Delta/\delta$ and k_g is multiplied by this ratio. For example, to look at filaments of size up to 500, we could let $\Delta/\delta = 5$ and then numerically solve roughly 100 equations instead of 500. Solving these numerically is easy if the lengths are greater than M. The problem is to connect this to the smaller fragments which are born from the actin dimers. The numerical strategy is to 'bootstrap' the process by using the single one-step equations for $x_2, x_3, \ldots, x_M$. We then use the rescaled equations for $x_{2M}, x_{3M}, \ldots$. The only trick left is to connect the 'small' steps with the 'big' steps, and that only occurs between x_M and x_{2M}. The equations that we have used for this procedure are shown in Appendix 3.

Finally, we rescale time in all the simulations relative to k_-, and thus all rate constants are relative to this rescaling of time. Thus, in the simulations below, one time unit corresponds to $1/k_- \approx 3$ s of real time.

7.1. ***Numerical results for the polymerization–fragmentation problem.*** In this section we investigate the equations derived in the preceding section. We consider the following three cases.

Case I (a, g fixed). Free gelsolin g, and free actin a, concentrations are artificially maintained at constant levels. (In this case, all the coefficients in the above differential equations are constant, and the equations are linear.) The system we simulate then consists of equations (6) and (10)–(14).

Case II (g, A_{total} fixed). Gelsolin is kept constant, but the free actin monomers are not held at a constant level. Since the total amount of actin A_{total} is fixed, the monomer concentration a is used up in polymerization. In this case, we have the additional equation for a, [equation (9)]. In the case of monomer depletion, the parameter $r = k_+a/k_-$ is not constant, but rather linearly proportional to a, and equations (6) and (9)–(14) are nonlinear.

Case III (A_{total} fixed). Both actin monomers and gelsolin are used up in the various reactions. In this case, we have the additional equation (8).

The parameters $\kappa = gk_g/k_-$ and $\iota = gk_{init}/k_-$ are then not constant: each one is proportional to the concentration of g (Table 1). The system to be simulated consists of equations (6) and (8)–(14)

In the simulations, we used a C language version of LSODE within XPP, a simulation package written by Ermentrout and available through the Internet. LSODE is a variable step-size solver for stiff ordinary differential equations. We set the relative and absolute tolerances to 10^{-8} and 10^{-7}, respectively, and the simulation time to a value of between 50 and 1000 time units, depending on the dynamics. Since time has been scaled in units of $(k_-)^{-1}$, one simulation time unit is equivalent to 3 s (using the value $k_- = 0.32$ s^{-1} from Table 1). The horizontal axis represents the length of the gelsolin-capped actin filaments in terms of the number of actin monomer units. Thus, 1 refers to the complex ga, 2 to gaa, and so on. The vertical axis represents either the concentration of the given complex in micromoles, or, in the case of exponentially growing concentrations, the relative abundance of various forms. Although the basic model was similar in all the cases described below, it is evident that the behavior of the system depends on further detailed assumptions about boundaries and subsidiary conditions.

7.1.1. *Results for Case I.* If the monomer pool is constant and $a > a_{crit}$, polymerization will continue without limit, and concentrations of all complexes will grow exponentially as we showed in Section 6. This type of behavior could take place over a limited time span in any biological setting: it could explain rapid growth phases when the cell is stimulated. Figure 1(a) shows the time evolution for a few small polymers. The larger ones never reach a substantial concentration due to the action of gelsolin. While the total mass grows exponentially, the average length quickly reaches a steady state. There is an initial essentially instantaneous jump to dimers and then a slow rise as polymerization and chopping equilibrate. This is shown in Fig. 1(b).

Even though the total mass of polymerized actin grows exponentially in the case shown by Fig. 1, the *relative proportions* of the various size-classes settles into a *stable size distribution*. We show this in Fig. 2(a) for a variety of concentrations of actin. The most prevalent size remains practically unchanged at about 2–4 monomers, but with larger actin concentrations the distribution becomes much broader, reflecting more filaments with large sizes. This is quantified by looking at the average lengths as a function of the actin concentration, shown in Fig 2(b). For actin concentrations that are sufficiently low, no growth occurs. Thereafter, the average length is a monotonic function of the actin concentration.

7.1.2. *Results for Case II.* When A_{total} is fixed, monomers are used up, so that a decreases. As we noted in Section 5.2, depending on whether there is fragmentation of the dimers or not, the steady-state distribution will consist only of ga or gaa polymers. However, the initial transients in this case are quite interesting. Figure 3(a) shows the time dependence of a variety of reactants in

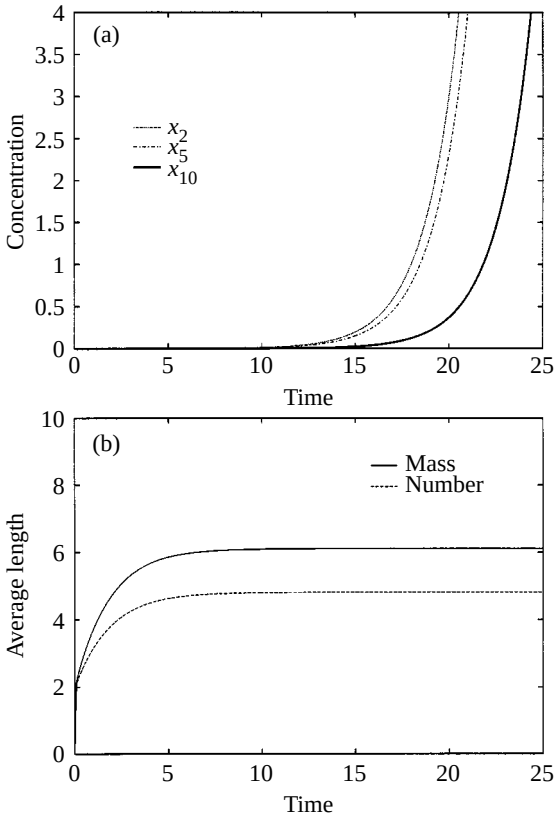

Figure 1. Case I. (a) Time course of polymerization/fragmentation with an (artificially) fixed pool of free actin monomers, $a = 2.0\ \mu$M and gelsolin fixed at $g = 0.01\ \mu$M. The vertical axis represents filament concentration in units of micromoles. Parameter values were: $k_+/k_- = 1.6\ \mu$M, $k_g/k_- = 15.0\ \mu\text{M}^{-1}$, $k_{init}/k_- = 0.0125\ \mu\text{M}^{-1}$, $k_{fast}/k_- = 100$, $k_2^-/k_- = 0.1$, $k_{init}/k_- = 0.05\ \mu\text{M}^{-1}$. The amount of polymerized actin grows exponentially and all size classes increase. However, the relative proportions of the various sizes settles into a stable distribution in which some classes dominate over others, as shown in Fig. 2. (b) Average length (in monomer equivalents) as a function of time. Though the mass of polymerized actin increases exponentially, the average length of the filaments (computed as mass average and number average) settles to some constant length, between four and six monomers long.

the early stages of the polymerization and chopping. Filaments quickly grow, with longer filaments reaching their peaks at times earlier than shorter filaments although these peaks are quite small. This apparently contradictory behavior is due to the action of the gelsolin and the slower kinetics of depolymerization. Essentially, the initial actin concentration is large enough to create growth. However, this is rapidly depleted and there is a slow depolymerization and chopping of the longer filaments. All that is ultimately left are the ga fragments (since k_2^- is nonzero). Note the slow growth of x_1 and the slow decay of x_2 once the initial transients are over. Figure 3(b) shows the average length (computed as the mass average and the number average). There is an initial growth followed

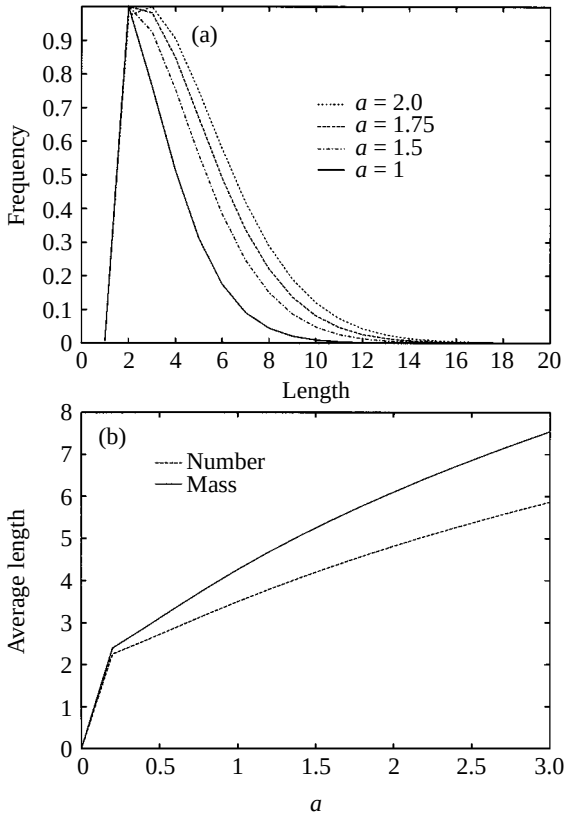

Figure 2. The effect of the actin monomer concentration on the relative abundance and average length of filaments. (a) The size distributions, normalized so that their peaks have a value of 1, tend to broaden toward longer lengths as the monomer concentration is increased. (b) The average length of the filaments (number and mass averages) as a function of the monomer concentration. (Sharp 'corners' are due to the fact that we looked at equally spaced increments of actin and there is a discontinuous jump from 0 to 2 as soon as there is a nonzero amount of actin.)

by a slower decay, ultimately terminating in only x_1 or x_2.

There are some subtle differences in the transients when the dimers (x_2) are prevented from depolymerizing. The temporal decay of the larger sizes such as x_3 is *faster* when there is *no breakdown* of the dimers. This result may be explained as follows. If dimers do not break down, the pool of actin monomers is depleted more quickly because monomers are not recycled from the dimer class. This means that the net trend for polymerization of filaments decreases, depolymerization becomes more dominant, and thus larger sizes decay more quickly.

7.1.3. *Results for Case III.* If we permit gelsolin to be consumed in the reaction (due to irreversible capping of filaments that it severs), the dynamics are only transiently affected by chopping and capping. Eventually, after most of the

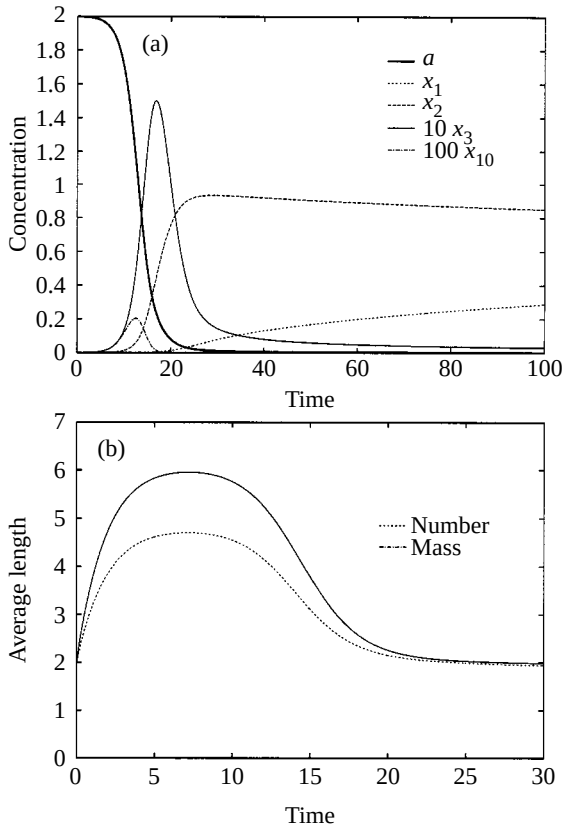

Figure 3. (a) Time course of polymerization/fragmentation in Case II, where the total amount of actin, $A_{total} = 2.0\ \mu$M is constant. Free actin, a, gets used up. Free gelsolin is held artificially fixed at $g = 0.01$. This means that filaments > 2 are continually being fragmented, so that they hardly build up to significant levels. Furthermore, once actin is complexed with gelsolin in the ga or gaa complex, it can no longer be added to the longer filaments. Thus, the depolymerization and the chopping result in only the smallest possible filaments remaining. The vertical axis is the filament number concentration in micromoles. The single actin complexes ga are ultimately all that remain. Parameter values were the same as those of Fig. 1, but with $A_{total} = 2.0\ \mu$M. (b) The average length of the filaments (in monomer units) at first increases via polymerization, and then through fragmentation and depolymerization it settles back to the smallest size. We show both the number average and the mass average length.

gelsolin has been bound to actin-barbed ends, there is no longer free gelsolin left to further interact with or fragment the filaments. In that case, polymerization/depolymerization (at the free pointed ends) will take over as the dominant process. However, the transients are quite interesting, as will be shown below.

The initial amount of gelsolin will determine the total number of filaments that can be formed, as gelsolin is here assumed to be responsible for actin filament initiation. This leads to the following situation: whether filaments can grow to large sizes will depend on how many filaments are available (proportional to the total amount of gelsolin supplied) and on the continued availability of monomers

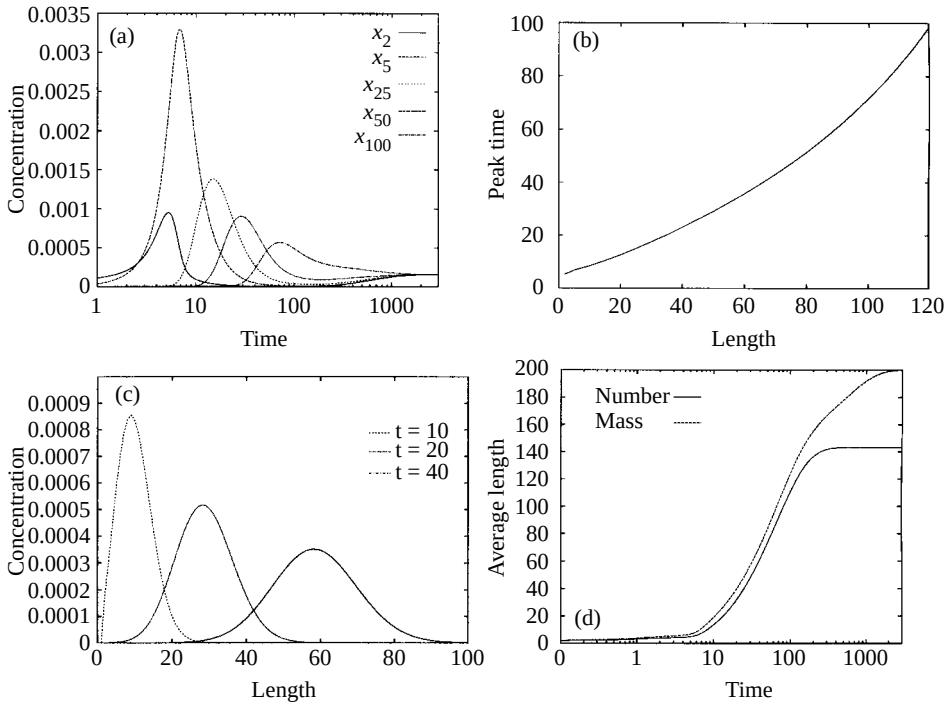

Figure 4. Time behavior in Case III, with gelsolin binding irreversibly in the reactions. Total amount of actin, $A_{total} = 2.0$, and total amount of gelsolin $G_{total} = 0.01$ μM are fixed, so that free monomers and gelsolin are depleted. Parameter values are the same as those for Fig. 1. (a) The time behavior of small filaments (up to 100 monomers long) until steady state is nearly reached. The transient behavior is bimodal with the first peak caused by polymerization of free actin and the second rise from depolymerization of long filaments. (b) The time of the first peak as a function of the size of the filament shows a less than exponential dependence. (c) Changes in the size distribution over the first 40 time units. Over a long period of time the distribution shifts back to an exponentially decreasing function of monomer length. (d) The average length over a long period of time (computed as number and mass average).

for these filaments to grow.

Figure 4(a) shows the transient behavior of the growth process over a long period of time. Each polymer concentration initially rises and then falls, and then, over a very slow timescale, rises again. This secondary rise time is due to the slow depolymerization reaction of the long filaments. (It is not due to the gelsolin fragmentation, which is negligible after a very short time since the gelsolin was largely depleted in the initiation reaction.) Note that asymptotically the concentrations of all the polymers appear to be very close to each other because the asymptotic decay rate, as given in the Appendix, is close to 1. (In fact it is 0.9985, so that the ratio x_{100}/x_2 is about 0.85, a small difference on this scale.)

The time at which filament concentration first peaks is not a simple function of the size (n) of the filament. (That is, it is not linear as in the case of a wave,

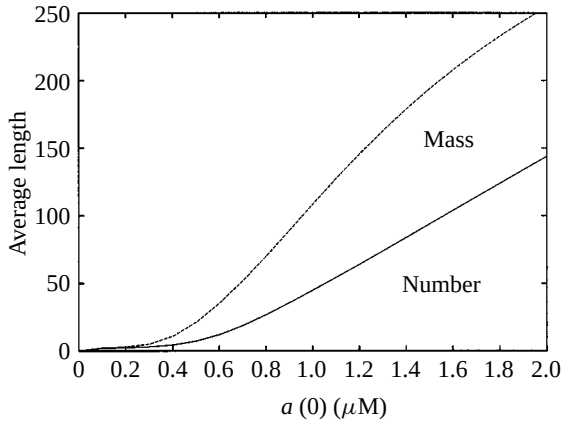

Figure 5. Average length as a function of the initial actin concentration. Note the 'threshold' at about 0.6 μM.

nor does it follow a diffusive time course.) Figure 4(b) shows that this function of size is shallower than an exponential. By looking at a variety of logarithmic plots, we have found that $t_{peak}(n) \sim e^{kn^p}$ where p lies between $\frac{1}{2}$ and $\frac{1}{3}$.

The length distributions, whose early evolution is shown in Fig. 4(c), evolve over time from a sharp peak at small sizes to a broader peak at larger sizes. This broad peak is washed out at very long times since the steady-state distribution is just an exponential decay in length (see Appendix 2). Figure 4(d) shows the average length (computed as mass and as number average) over a long period of time. The length average saturates at about 140 as predicted by approximation (17) given in section 5. Note that for the parameters used in the simulation,

$$\bar{\ell} \approx \frac{2 - 1/1.6}{0.01} = 137.5.$$

The mass average is computed to be about 250, higher than that found in the numerical simulation. (This is may be due to the finite cut-off size in the numerical simulations. Simulations with larger cut-off showed a mass average of close to 250, in agreement with the full model.)

Lower actin concentrations result in a similar picture—transient rises followed by settling into an exponential steady-state profile. However, there is a threshold-like behavior of the average length as the actin concentration is increased from a low to a high concentration. Figure 5 shows the steady-state average length as a function of the total actin for initial gelsolin fixed at $g(0) = 0.01$. Note the essentially flat small average lengths up to $a(0) \approx 0.6$ followed by nearly linear growth from that point. The threshold is just k_-/k_+; below this the dimers occupy most of the total actin; above this the fraction of actin occupied by a longer filament increases.

8. Discussion and Comparison with Literature

The overall reactions of actin and gelsolin were modeled using chemical kinetics (Ditsch and Wegner, 1994). They described the equilibrium level of actin in polymerized form when nucleation is mediated by gelsolin, but omitted the details of how fragmentation influences the length distribution. Because the number of filaments that form are assumed to be the same as the number of gelsolin nuclei in their paper, it is not essential to know the length distribution to determine how much actin is in polymerized form. The time rate of formation of gelsolin-actin complexes has also been discussed (Selve and Wegner, 1986). However, knowledge of the length distribution is of interest in its own right, and as an input for studies attempting to understand the spatial distribution and dynamics of actin cytoskeletal networks.

The problem of gelsolin-mediated nucleation and pointed-end polymerization is described briefly in an appendix of a paper about the liquid-crystalline order of F-actin (Coppin and Leavis, 1992). (Fragmentation is neglected, and the equations are solved numerically with one set of parameter values.) The effect of capping proteins on length distributions has been discussed using free-energy arguments (Madden and Herzfeld, 1994).

Experimental size distributions of actin filaments polymerized in the presence of gelsolin were determined by electron-microscopy and are shown in a paper by (Janmey *et al.*, 1986). The authors state that these distributions are similar to those obtained in the absence of gelsolin, but the distributions shown in their Figure 1 appear to have some internal maxima, similar to those found in our simulations. Spontaneous breakage (and/or annealing) may have been the cause of this result. Calculations of the weight-average and number-average length are given. To our knowledge, a detailed theoretical treatment of the fragmentation-polymerization-capping process, and its effect on filament length distributions appears for the first time in the present paper.

The results of this paper can be summarized briefly as follows:

(i) The combined effects of polymerization and fragmentation can, under certain circumstances, give rise to transient length distributions in which some intermediate size class is most prevalent, i.e., distributions with peaks. However, steady state distributions are always monotone.

(ii) The case of constant total actin available (A_{total} constant; here referred to as the '*in vitro* case') and the case of constant free actin monomer pool (a constant; '*in vivo* case') give different results. The model is linear in the second case, and nonlinear in the first. The main difference is in the *in vivo* case, all filament sizes grow without bound.

(iii) Seemingly small changes in the assumptions can have major effects on the behavior of the models. For example, making the nuclei (e.g., dimers) more or less stable to break-up can completely change both the dynamics, and the resulting size distribution, as it determines replenishment of the

pool of monomers ''fueling" further growth.

(iv) A fragmenting agent that gets 'used up' or irreversibly attached to actin filaments (as is the case in gelsolin) leads to drastically different resulting behavior than one that gets recycled. In the former case, the process is ultimately dominated by polymerization after all the gelsolin has been bound. This suggests that agents that uncap gelsolin from actin filaments are as important in determining length distributions as is the gelsolin itself. (This effect has not been investigated in detail, and bears further study.)

(v) The fact that gelsolin initiates actin filaments 'essentially' from actin monomers (since the formation of a gaa complex is very fast once a ga complex is formed) means that the whole process of filament growth and fragmentation in the low gelsolin case follows linear kinetics. It is important to stress that this is not the case if actin initiation occurs in the absence of gelsolin (three or possibly four monomers are then needed to form a nucleus, leading to nonlinear initiation kinetics). The fact that nucleation is linear in the presence of gelsolin allowed great simplification, as linear algebra methods completely characterize the steady state behavior.

Our model for gelsolin is still in a preliminary form, as we have not yet included the effects of ionic composition, of calcium, and of many other factors in the cell that could modulate the various reactions.

With the information emerging on the structure, function, sensitivity, and effects of gelsolin and its cousins, an intriguing picture is emerging about the way that the cell's cytoskeletal machinery transduces and responds to chemical signals. It appears that a decrease in membrane-associated PIPs and an increase in local calcium concentration (as may occur, for example, in a calcium wave) will cause gelsolin to cut and cap actin filaments locally. Since gelsolin remains attached to the barbed ends of the filaments, and has a very slow off-rate, the growth by polymerization is limited, until a second step. If PIP or PIP_2 subsequently increases, the gelsolin caps fall off, and the filaments can undergo rapid polymerization at all the newly created barbed ends. In this way, a sensitive regulation of the extent and location of cytoskeletal growth can be achieved in the cell. Recent research aims to explore how actin-binding proteins such as severin affect motility by studying mutants defective in the gene.

ACKNOWLEDGMENTS

The authors would like to thank Alex Mogilner for reading and commenting on a draft of the manuscript. We are grateful for the encouragement and many suggestions provided by the anonymous reviewers. LEK is supported by a Canadian NSERC operating grant OGPIN 021. G. Bard Ermentrout is supported by National Science Foundation (US) grant number DMS-9626728. LEK is currently a member of the "Crisis Points" group, funded by the Peter Wall Institute at UBC.

APPENDIX 1: FURTHER REFERENCES FOR ACTIN FRAGMENTING PROTEINS

- **General references** (Hartwig *et al.*, 1990; Hartwig and Kwiatkowski, 1991; Schoepper and Wegner, 1992; Ditsch and Wegner, 1994, 1995; Teubner *et al.*, 1994).
- **Structural Comparisons** of proteins in the gelsolin family: (Andrè *et al.*, 1988; Janmey and Matsudaira, 1988; Yin *et al.*, 1990; Barron-Casella *et al.*, 1995; Lueck *et al.*, 1995; Schnuchel *et al.*, 1995).
- **Functional comparisons** of proteins in the gelsolin family: (Hartwig and Kwiatkowski, 1991) and for villin: (Janmey and Matsudaira, 1988), severin: (Yin *et al.*, 1990), scinderin: (Del Castillo *et al.*, 1990), brevin: (Doi and Frieden, 1984), fragmin: (Furuhasi and Hatano, 1990),β-actinin: (Doi and Frieden, 1984; Andrè *et al.*, 1988; Yin *et al.*, 1990).
- **Ionic sensitivity** of gelsolin to calcium: (Howard *et al.*, 1990; Yin *et al.*, 1990; Hartwig and Kwiatkowski, 1991) of villin (Fath and Burgess, 1995), of fragmin: (Furuhasi and Hatano, 1990); of villin to Potassium: (Janmey and Matsudaira, 1988); of gelsolin to magnesium (Laham *et al.*, 1993).
- **Downregulation** and expression of gelsolin in cell development: (Kwiatkowski, 1988; Vandekerckhove *et al.*, 1990; Hartwig and Kwiatkowski, 1991)
- **Defective mutants** for severin: (Schindl *et al.*, 1995; Weber *et al.*, 1995)

APPENDIX 2: SOLVING FOR THE SIZE DISTRIBUTION IN THE STEADY STATE

We solve for the constant B and for the steady state free monomer concentration a so that the size distribution in the gelsolin-free steady state will be determined.

Since $g(\infty) = 0$, equation (15) implies that:

$$g(0) = \sum_{j=2}^{N} x_j = B\frac{r^2 - r^{N-1}}{1-r}$$

where $r \equiv k_+a/k_- < 1$ The conservation of total actin, equation (16) implies that $a(0) - a = \sum_{j=2}^{N} jx_j$ so that

$$k_+a(0)/k_- - r = \frac{B}{(1-r)^2}\left(r^2(2-r) - r^{N+1}((N+1)(1-r)+r)\right).$$

Thus, we solve the first equation for B and the second for r. For simplicity, consider the case $N \to \infty$. This means we have to solve:

$$g(0) = B\frac{r^2}{1-r} \tag{32}$$

$$k_+a(0)/k_- - r = \frac{Br^2}{1-r}\left(1 + \frac{1}{1-r}\right) = g(0)\left(1 + \frac{1}{1-r}\right) \tag{33}$$

where we have used (32) to simplify (33). Now we can see that if there is enough initial actin or if the initial gelsolin is small enough, then (33) can be solved for a unique value of r between 0 and 1. To see this note that the left hand side is a linearly decreasing function with a maximum value $k_+a(0)/k_-$ at $r = 0$. The right-hand side is monotonically increasing with a minimum $2g(0)$ at $r = 0$. Since the right hand side tends to infinity as $r \to 1^-$ this means that there will be a root as long as

$$k_+a(0)/k_- > 2g(0).$$

Since we have assumed that the gelsolin concentration is small, this is a reasonable constraint. This analysis shows that **the steady state distribution is always exponential** with the most numerous filaments being the dimers. There are no peaks in the distribution; it is monotonic. However, the mean length of the filaments is not 2 but rather a larger number that depends on the relative concentrations of gelsolin and actin. In fact, we can write down the solution to (33). Let $\alpha = k_+a(0)/k_-$. Then

$$r = \frac{1}{2}\left(\alpha + 1 - g(0) - \sqrt{(\alpha-1)^2 + g(0)^2 + g(0)(6-2\alpha)}\right).$$

This unwieldy expression can be approximated for small $g(0)$ by

$$r \approx 1 - \frac{g(0)}{\alpha - 1}.$$

APPENDIX 3: SCALING THE EQUATIONS FOR NUMERICAL SIMULATIONS

The following equations were used to simulate the model in the situation where a length of hundreds of monomers was desired:

$$\begin{aligned}\frac{dx_2}{dt} &= k_{init}a + k_-x_3 - (k_+a + k_{-,dimer})x_2 \\ &\quad +2gk_g\left(\sum_{k=2}^{M} x_k + M\sum_{k=2}^{N} x_{kM}\right) \qquad (34)\\ \frac{dx_j}{dt} &= r(x_{j-1} - x_j) + (x_{j+1} - x_j) - \kappa(j-1)x_j \\ &\quad +2\kappa\left(\sum_{k=j+1}^{M} x_k + M\sum_{k=2}^{N} x_{kM}\right) \qquad (35)\\ \frac{dx_M}{dt} &= r(x_{M-1} - c_2x_M/M) + (c_1x_{2M}/M - x_M)\end{aligned}$$

$$+\kappa\left((M-1)x_M + 2M\sum_{k=2}^{N} x_{kM}\right) \tag{36}$$

$$\frac{dx_{2M}}{dt} = r(c_2 x_M - x_{2M})/M + (x_{3M} - x_{2M})/M$$

$$+\kappa\left(-(2M-1)x_{2M} + M\sum_{k=3}^{N} x_{kM}\right) \tag{37}$$

$$\frac{dx_{jM}}{dt} = r(x_{(j-1)M} - x_{jM})/M + (x_{(j+1)M} - x_{jM})$$

$$+\kappa\left(-(jM-1)x_{jM} + M\sum_{k=j+1}^{N} x_{kM}\right) \tag{38}$$

Here c_1, c_2 are ''fudge factors" usually set to 1 but which could be scaled differently to get better agreement with the ''full" model.

REFERENCES

Aizawa, H., K. Sutoh and I. Yahara (1996). Overexpression of cofilin stimulates bundling of actin filaments, membrane ruffling, and cell movement in dictyostelium. *J. Cell Biol.* **132**, 335–344.

Andrè, E., F. Lottspeich, M. Schleicher and A. Noegel (1988). Severin, gelsolin, and villin share a homologous sequence in regions presumed to contain F-actin severing domains. *J. Biol. Chem.* **263**, 722–727.

Vasconcellos, C., P. G. Allen, M. E. Wohl, J. M. Drazen, P. A. Janmey and T. P. Stossel (1994). Reduction in viscosity of cystic fibrosis sputum in vitro by gelsolin. *Science* **263**, 969–971.

Barron-Casella, E. A., M. A. Torres, S. W. Scherer, H. H. Q. Heng, L. C. Tsui and J. F. Casella (1995). Sequence analysis and chromosomal localization of human cap Z: Conserved residues within the actin-binding domain may link cap Z to gelsolin/severin and profilin protein families. *J. Biol Chem.* **270**, 21472–21479.

Biogen (1996). WWW Press Release, Cambridge, MA, Biogen Announces begining of phase I clinical trial of gelsolin as potential treatment for respiratory diseases. `http://www.biogen.com/frame/company/index.html`

Coppin, C. M. and P. Leavis (1992). Quantitation of liquid-crystaline ordering in F-actin solutions. *Biophys J.* **63**, 794–807.

Del Castillo, A. R., S. Lemaire, L. Tchakarov, M. Jeyapragasan, J. Doucet, M. Vitale and J. Trifarö (1990). Chromaffin cell scinderin, a novel calcium-dependent actin filament-severing protein. *EMBO J.* **9**, 43–52.

Ditsch, A. and A. Wegner (1994). Nucleation of actin polymerization by gelsolin. *Eur. J. Biochem.* **224**, 223–227.

Ditsch, A. and A. Wegner (1995). Two low-affinity Ca++ binding sites of gelsolin that regulate association with actin filaments. *Eur. J. Biochem.* **229**, 512–516.

Doi, Y. and C. Frieden (1984). Actin polymerization: The effect of brevin on filament size and rate of polymerization. *J. Biol. Chem.* **259**, 11868–11875.

Edelstein-Keshet, L. and G. B. Ermentrout (1998). Models for the length distribution of actin filaments: I. Simple polymerization and fragmentation acting alone. *Bull. Math. Biol.* **60**, 449–475.

Fath, K. R. and D. R. Burgess (1995). Not actin alone. *Curr. Biol.* **5**, 591–593

Furuhasi, K. and S. Hatano (1990). Control of actin filament length by phosphorylation of fragmin-actin complex. *J. Cell Biol.* **111**, 1081–1087

Hartwig, J. H., D. Brown, D. A. Ausiello, T. P. Stossel and L. Orci (1990). Polarization of gelsolin and actin binding protein in kidney epithelial cells. *J. Histochem. Cytochem.* **38**, 1145–1153.

Hartwig, J. H. and D. J. Kwiatkowski (1991). Actin binding proteins. *Curr. Opin. Cell Biol.* **3**, 87–97.

Hawkins, M., B. Pope, S. K. Maciver and A. G. Weeds (1993). Human actin depolymerizing factor mediates a pH-sensitive destruction of actin filaments. *Biochem.* **32**, 9985–9993.

Hayden, S. M., P. Miller, A. Brauweiler and J. R. Bamburg (1993). Analysis of the interactions of actin depolymerizing factor with G- and F-actin. *Biochem.* **32**, 9994–10004.

Horn, R. A. and C. R. Johnson (1985). *Matrix Analysis*, Cambridge: Cambridge University Press.

Howard, T., C. Chaponnier, H. Yin and T. Stossel (1990). Gelsolin–actin interaction and actin polymerization in human neutrophils. *J. Cell Biol.* **110**, 1983–1991.

Janmey, P. A. and P. T. Matsudaira (1988). Functional comparison of vilin and gelsolin. *J. Biol. Chem.* **263**, 16738–16743.

Janmey, P. A., J. Peetermans, K. S. Zaner, T. P. Stossel and T. Tanaka (1986). Structure and mobility of actin filaments as measured by quasielectric light scattering, viscometry and electron microscopy. *J. Biol. Chem.* **261**, 8357–8362.

Kwiatkowski, D. J. (1988). Predominant induction of gelsolin and actin-binding protein during myeloid differentiation. *J. Biol. Chem.* **263**, 13857–13862.

Laham, L. E., J. A. Lamb, P. G. Allen and P. A. Janmey (1993). Selective binding of gelsolin to actin monomers containing ADP. *J. Biol. Chem.* **268**, 14202–14207.

Lauffenburger, D. A. and A. F. Horowitz (1996), Cell migration: a physically integrated molecular process. *Cell* **84**, 359–369.

Lueck, A., J. D'Haese and H. Hinssen (1995). A gelsolin-related protein from lobster muscle: cloning, sequence analysis and expression. *Biochem. J.* **305**, 767–775.

Maciver, S. K., H. G. Zot and T. D. Pollard (1991). Characterization of actin filament severing by actophorin from Acanthamoeba castellanii. *J. Cell Biol.* **115**, 1611–1620.

Madden, T. L. and J. Herzfeld (1994). Crowding-induced organization of cytoskeletal elements: II. dissolution of spontaneously formed filament bundles by capping proteins. *J. Cell Biol.* **126**, 169–174.

McGough, A. (1997). Structural Studies of Gelsolin: Actin Interactions, Baylor College of Medicine, Houston, `http://dali.bcm.tmc.edu/~amy/Gelsolin.html`

Mitchison, T. J. and L. Cramer (1996). Actin-based cell motility and cell locomotion. *Cell* **84**, 371–379.

Moon, A. and D. G. Drubin (1995). The ADF/cofilin proteins: Stimulus-responsive modulators of actin dynamics. *Mol. Biol. Cell* **6**, 1423–1431.

Redmond, T. and S. H. Zigmond (1993). Distribution of F-actin elongation sites in lysed polymorphonuclear leukocytes parallels the distribution of endogenous F-actin. *Cell Motil. Cytoskel.* **26**, 1–18.

Schindl, M., E. Wallraff, B. Deubzer, W. Witke, G. Gerisch and E. Sackmann (1995).

Cell-substrate interactions and locomotion of dictyostelium wild-type and mutants defective in three cytoskeletal proteins: a study using quantitative reflection interference contrast microscopy. *Biophys. J.* **68**, 1177–1190.

Schnuchel, A., R. Wiltscheck, L. Eichinger, M. Schleicher and T. A. Holak (1995). Structure of severin domain in solution. *J. Mol. Biol.* **247**, 21–27.

Schoepper, B. and A. Wegner (1991). Rate constants and equilibrium constants for binding of actin to the 1:1 gelsolin-actin complex. *Eur J. Biochem.* **202**, 1127–1131.

Schoepper, B. and A. Wegner (1992). Gelsolin binds to polymeric actin at a low rate. *J. Biol. Chem.* **267**, 13924–13927.

Selve, N. and A. Wegner (1986). Rate of treadmilling of actin filaments in vitro. *J. Mol. Biol.* **187**, 627–631.

Selve, N. and A. Wegner (1987). pH-dependentrate of formation of the gelsolin-actin complex from gelsolin and monomeric actin. *Eur. J. Biochem.* **168**, 111–115.

Stossel, T. P. (1994). Gelsolin: another potential therapy for CF Sputum. `http://www.ai.mit.edu/people/mernst/cf/cfri`

Teubner, A., I. Sobek-Klocke, H. Hinssen and U. Eichenlaub-Ritter (1994). Distribution of gelsolin in mouse ovary. *Cell Tissue Research* **276**, 535–544.

Theriot, J. A. (1994). Actin filament dynamics in cell motility, in *Actin: Biophysics, Biochemistry, and Cell Biology*, J. E. Estes and P. J. Higgins (Eds), New York: Plenum Press, pp. 133–145.

Vandekerckhove, J., G. Bauw, K. Vancompernolle, B. Honoré and J. Celis (1990). Comparative two-dimensional gel analysis and microsequencing identifies gelsolin as one of the most prominent downregulated markers of transformed human fibroblast and epithelial cells. *J. Cell Biol.* **111**, 95–102

Weber, I., E. Walraff, R. Albrecht and G. Gerisch (1995). Motility and substratum adhesion of *dictyostelium* wild-type and cytoskeletal mutant cells: a study by RICM/bright-field double-view image analysis. *J. Cell Sci.* **108**, 1519–1530.

Yin, H. L., P. A. Janmey and M. Schleicher (1990). Severin is a gelsolin prototype. *FEBS Lett.* **264**, 78–80.

Zigmond, S. H. (1993). Recent quantitative studies of actin filament turnover during cell locomotion. *Cell Motil. Cytoskel.* **25**, 309–316.

Received 24 October 1996 and accepted 25 June 1997